Sensitivity Measurements for Two West Mountain Observatory CCDs and Exposure Times for Observing Exoplanets

Andrew Phillip DeWitt

A senior thesis submitted to the faculty of
Brigham Young University
in partial fulfillment of the requirements for the degree of

Bachelor of Science

Denise Stephens, Advisor

Department of Physics and Astronomy

Brigham Young University

August 2011

ABSTRACT

Sensitivity Measurements for Two West Mountain Observatory CCDs
and Exposure Times for Observing Exoplanets

Andrew Phillip DeWitt
Department of Physics and Astronomy
Bachelor of Science

Magnitude sensitivities and zero point values are presented for the Kodak KAF-09000 and Fairchild 3041-UV CCDs mounted on the 0.9m telescope at BYU's West Mountain Observatory. Sensitivities and zero points presented for the KAF-09000 and 3041-UV CCDs are given in the Johnson V, B, R, I and Johnson V, B, R filters, respectively. These values were calculated by performing aperture photometry on the open cluster NGC 188 and Landolt standard stars SA 110 using an aperture radius of 8 pixels. The sensitivities provide a starting point for determining exposure times to observe exoplanet candidates discovered by the NASA Kepler Mission and other stellar objects with short-term variability.

Keywords: WMO, exoplanets, sensitivities, zero points, variable star, CCD, aperture photometry, NGC 188, SA 110

ACKNOWLEDGMENTS

I want to thank all those who have helped in the development of this thesis. Dr. Stephens, thank you for teaching me so much about exoplanets and for guiding me in solving the mystery of why the sensitivities were not improving with integration time. Joseph Rawlins, thank you for doing the photometry and calculating the zero points that made this thesis possible. I want to thank my wife and daughter for their support as I spent time away from home finishing my research. Thanks to the software developers of Mathematica 8 for making a program that generates awesome plots and figures. Finally, I want to thank my father for helping me revise my thesis.

Contents

List of Figures

List of Tables

Chapter 1

Introduction

1.1 Overview

The frequency and exposure time of observations of stellar objects with short-term variability can affect the resolution of the resulting magnitudes vs. time plot (i.e light curve). The frequency of images and exposure times of the charge coupled device (CCD) need to be determined so that there are enough data points to see features of interest but with small enough errors that those features are not drowned in the noise of the data. The method of discovering exosolar planets (exoplanets) using planetary transits requires the study of light variability in the exoplanet's host star. Since BYU has recently begun studying potential exosolar planets, there was a need to calculate how sensitive the CCDs are at West Mountain Observatory (WMO) in order to determine observational exposure times. The sensitivities of a CCD are measures of how accurate the CCD is at various exposure times and magnitudes. This thesis will present the methods used to calculate these sensitivities, the results of those calculations, and a sample application of those results.

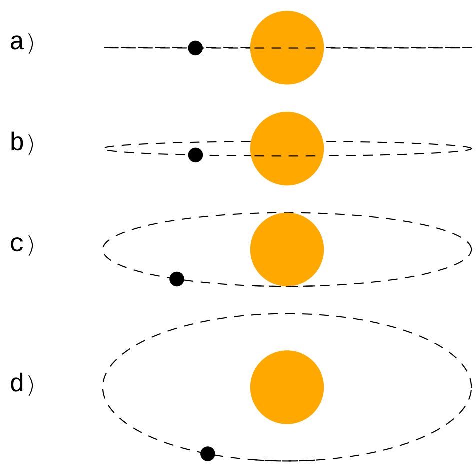

Figure 1.1 A host star (represented by the orange disk) and its planet (represented by the smaller black disk) are shown in various orbit orientations. A exoplanetary transit is only viewable from Earth if the planet crosses in front of the host star. Orbit a) is edge on so a transit is visible. Orbit b) is slightly off edge, but still passes in from of the star. Orbit c) is most inclined an orbit can be and have the transit still visible. Orbit d) is so inclined that the planet never eclipses its host star.

1.2 Background

1.2.1 Exoplanetary Transits

An exoplanets is a planet that orbits a star other than our own. Exoplanets are currently a hotbed of astronomical research because they potentially hold the key to helping us understand how solar systems form and may help us in our search for life beyond Earth. A common technique for finding exoplanets is the planetary transit method. This method of finding exoplanets is achieved by noting the effect a planet has on the brightness of the star it orbits. If an exoplanet has the right orbit (see Fig. 1.1) with respect to the Earth (i.e., edge on), as the planet crosses between the star and Earth (i.e., as it transits), the exoplanet will eclipse some of the light from its host star. This eclipse will cause a slight drop in the magnitude of the star. The resulting light curve can be observed and contains information about the exoplanet's orbital period, orbital radius, size, and temperature (if the spectral type of the host star is known).

1.2.2 NASA Kepler Mission

In March 2009, NASA launched the Kepler telescope into space. Continuously observing the magnitudes of over 100,000 stars, the Kepler satellite is able to detect periodic dips in brightness that may be caused by exoplanets. In 2011, the NASA Kepler Mission published a paper announcing its discovery of 1,235 exoplanet candidates (Borucki et al. 2011). To confirm whether these were exoplanets, NASA released a list of these candidates for public follow up observations from ground-based telescopes. Using this list of planet candidates, BYU has selected targets on which to perform some of these follow up observations. In order to observe these targets with sufficient accuracy, sensitivity measurements for the WMO 0.9m telescope were needed.

Chapter 2

Experimental Methods

2.1 Observations

Sets of observations were taken with the 0.9m telescope at WMO using the Kodak KAF-09000 (3k$\times$3k pixel) CCD and the Fairchild 3041-UV (2k$\times$2k) CCD. Each set of observations included images of the open star cluster NGC 188 and images of Landolt standard star field SA 110 (Landolt 1973). The observations of NGC 188 were taken in order to provide a good distribution of high to low magnitude stars. This distribution would make it possible to determine sensitivities and integration times for different star magnitudes. The Landolt standard star field would provide reliable zero points for performing photometry on the stars in the cluster. (See Sec. 2.4.)

Observers took images with the KAF-09000 CCD in July 2010 and with the Fairchild 3041-UV in September 2010. Images were taken with the KAF-09000 CCD using the Johnson V, B, I, and R filters. Images with the Fairchild 3041-UV were taken using the Johnson B, V, and R filters. The KAF-09000 and 3041-UV CCDs mounted on the 0.9m WMO telescope produced a plate scale of $0.49\frac{\text{arcsec}}{\text{pixel}}$ and $0.61\frac{\text{arcsec}}{\text{pixel}}$, respectively. Images of NGC 188 were taken with various exposure times in order to see how errors in magnitude changed as the exposure times increased.

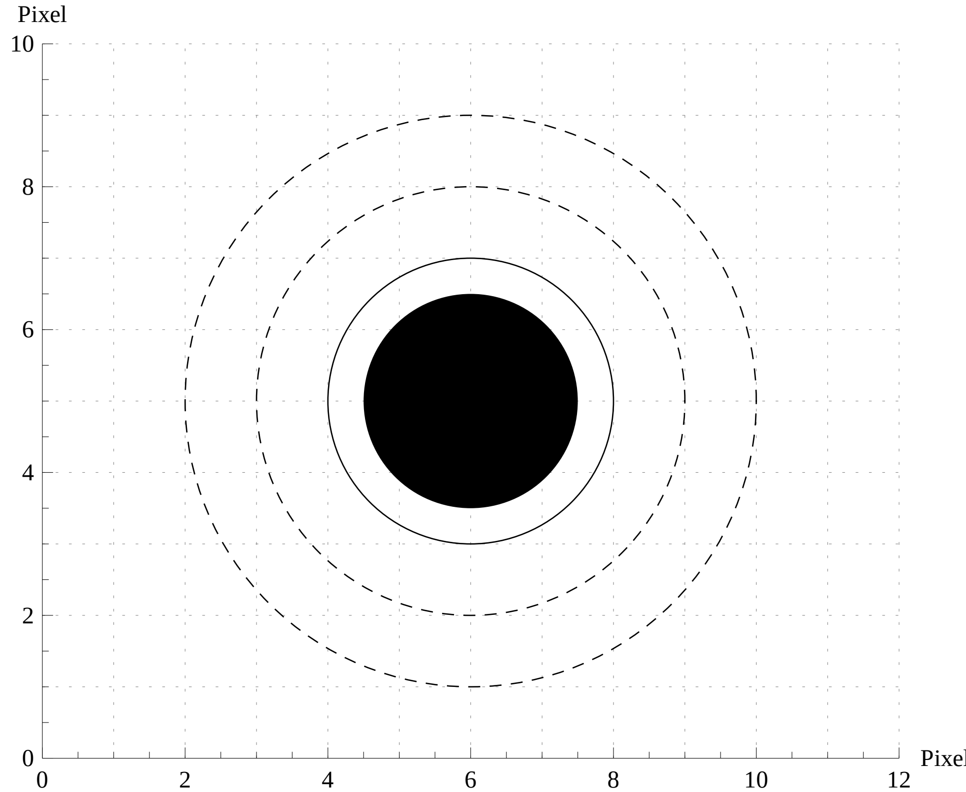

Figure 2.1 An aperture (represented by the solid circle) is drawn around a star (represented by the center disk) to find N_{tot}. The annulus (represented by the dashed line) is drawn around the aperture to find m_{sky} (Howell 2006).

The exposure times were 60s, 120s, 240s, 480s, and 960s. Both images of the Landolt standard star field and NGC 188 were reduced using standard IRAF (Tody 1993) zero, dark, and flat correction techniques.

2.2 Aperture Photometry

Aperture photometry is a method of analyzing images to find stellar magnitudes. It is done by adding pixel counts in a circular aperture of radius R [pixels] around a star. Since the sky has a certain brightness, an annulus is drawn (see Fig. 2.1) around the star's aperture to find an average value for pixel counts that are caused by the brightness of the sky. To obtain the number of pixel counts from the star this equation was used

$$N_{\text{star}} = N_{\text{tot}} - m_{\text{sky}} * A \tag{2.1}$$

where N_{star} is the pixel counts caused by the star's light, N_{tot} is the total pixel counts within the aperture, m_{sky} is the average counts per pixel due to the sky (found from the annulus), and A is the area of the aperture. The error in N_{star} is given by

$$\sigma^2_{N_{\text{star}}} = \sigma^2_{N_{\text{tot}}} + \left(A * \sigma_{m_{\text{sky}}}\right)^2 \tag{2.2}$$

where $\sigma^2_{N_{\text{tot}}} = N_{\text{tot}}$ because pixel counts follow a Poisson distribution. By multiplying N_{star} by the gain (G) of the CCD, the number of photons that came from the star can be calculated. The number of photons coming from the star is called the signal (S).

As the aperture radius increases, the signal will increase up to a certain point where it accounts for most of the light coming from the star. As the aperture continues to increases beyond that point, the signal will not increase significantly, but the noise in the signal will continue to increase. The best aperture size to choose for photometry is one that will capture all the signal from the star and include as little noise as possible from the surrounding pixels.

To find this aperture size aperture photometry was performed on several bright stars in each filter of the NGC 188 field using aperture radii from 1.5 to 10 pixels in .5 pixel steps. The resulting values of N_{star} were then plotted with respect to aperture (see Fig. 2.2) showing that an aperture radius of 8 pixels collected most of the counts from the star. At an aperture radius of 8 pixels, it was seen that N_{star} began to flatten out. At a larger aperture, the noise cost would have been too high for any star counts to be obtained.

Having chosen the aperture size, magnitudes could then be obtained from the stars using the equation

$$M = -2.5 \log_{10}\left(\frac{S}{t}\right) + M_z, \tag{2.3}$$

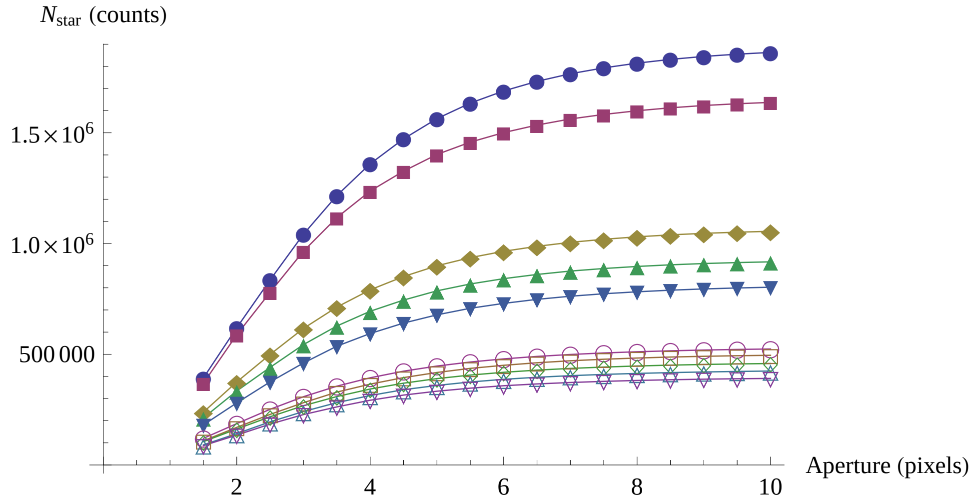

Figure 2.2 To find the right aperture size N_{star} is plotted with respect to aperture size for several bright stars in NGC 188. Each of the lines represents a different star. Notice how the star counts flatten off around aperture 8. (Plot made from the V filter KAF-09000 image data)

where M is the magnitude, S is the signal from an 8 pixel aperture radius, t is the integration time, and M_z is the zero point magnitude.

2.3 Sky Values

When performing aperture photometry on the stars in the NGC 188 field it was noticed that the magnitudes of many of the stars changed as the CCD exposure time increased. It was also noticed that the signal-to-noise ratio (S/N) did not increase as expected with increased exposure time. The longer the CCD was exposed, more stars appeared in the field because the star cluster NGC 188 is a crowded field. As more stars began to appear, stars began to add their pixel counts to the sky annulus (see Fig. 2.3). This was changing the values of m_{sky} and σ_{sky}. As the exposure time increased, these values changed enough to significantly affect individual stellar magnitudes and errors in those magnitudes.

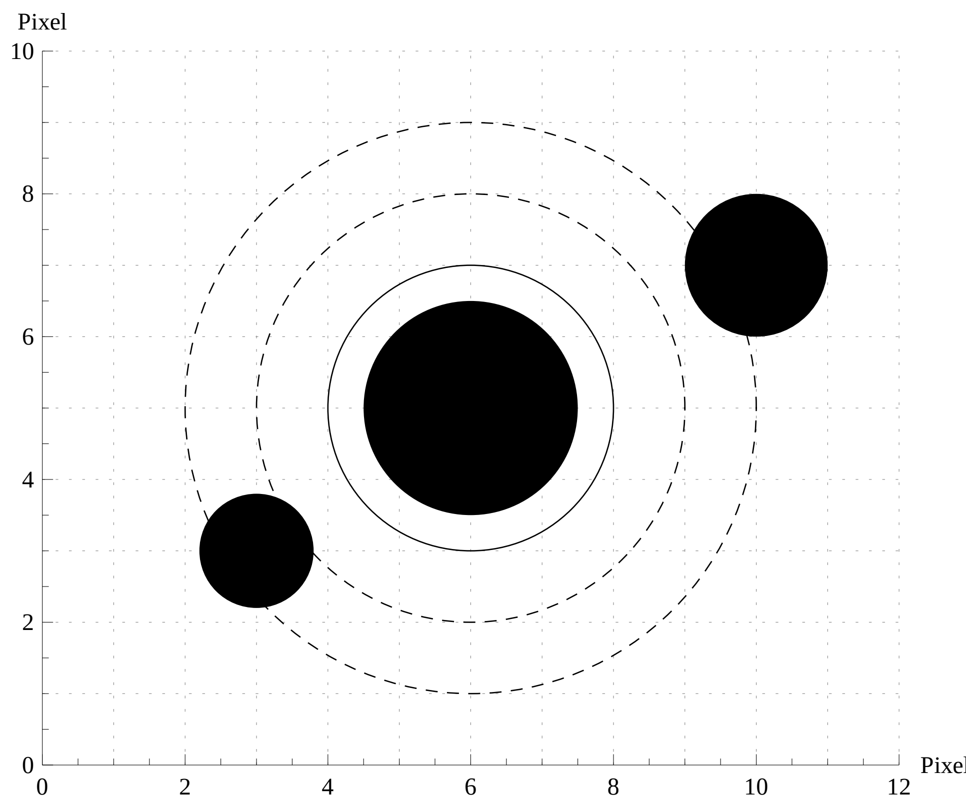

Figure 2.3 In the longer exposure times, the field got crowded as stars began to appear. The field go so crowded that stars were within the the sky annulus (represented by the dashed line), thus changing the value of the background sky (m_{sky}).

In order to remove the effects of the crowded field, manual measurements were made of $m_{\rm sky}$ for each image. To make these measurements, 5 × 5 pixel boxes were selected in regions without any stars and the average pixel count ($m_{\rm sky}$) and standard deviation ($\sigma^2_{m_{\rm sky}}$) of those 25 pixels were found. Doing this six times for each image, a weighted average was taken using the equations

$$\langle m_{\rm sky} \rangle = \frac{\sum_{i=1}^{n} \frac{m_{\rm sky}}{\sigma^2_{m_{\rm sky}}}}{\sum_{i=1}^{n} \frac{1}{\sigma^2_{m_{\rm sky}}}} \tag{2.4}$$

and

$$\sigma^2_{\langle < m_{\rm sky} \rangle} = \frac{1}{\sum_{i=1}^{N} \frac{1}{\sigma^2_{m_{\rm sky}}}}. \tag{2.5}$$

Values for $m_{\rm sky}$ and $\sigma_{m_{\rm sky}}$ were found that we could then be applied to stars in each image.

2.4 Zero Points

In order to use equation 2.3 to assign magnitudes to stars in the NGC 188 field, it was necessary to find the value of M_z (i.e., the zero point) for each filter-CCD combination. To determine the zero points, standard aperture photometry (i.e., using a sky annulus) was performed on the Landolt standard stars. Using those signals and rearranging equation 2.3 into

$$M_z = M + 2.5 \log_{10} \left(\frac{S_8}{t} \right) \tag{2.6}$$

M_z could be found since the magnitudes M are known values for standard stars (Landolt 1973). Using the standard stars, M_z was found for each star in each image. Taking an average of the value of M_z for each filter, zero point values were obtained for each filter-CCD combination. With these zero points the true magnitudes of the stars in the NGC 188 could then be determined. With true magnitudes the error as a function of magnitude could be studied.

2.5 Aperture Correction

In section 2.2 it was discussed that an aperture of radius 8 captured all of the star's light. This is true for both bright and faint stars; however, for fainter stars the signal-to-noise ratio gets worse for pixels further away from the central bright pixel. In order to reduce the noise that occurs in faint stars near the edge of a radius 8 aperture, an aperture correction was created that would map the pixel counts (N_{star}) from an aperture radius of 3 pixels to an aperture radius of 8 pixels. The correction allowed the stars' signals at an aperture of radius 8 to be obtained without including the extra error.

To create an aperture correction a set of bright stars was chosen for each CCD to define a relationship between the star pixel counts at aperture 8 ($N_{\text{star},8}$) and at an aperture of 3 ($N_{\text{star},3}$). Bright stars were chosen because they have a strong linear relationship between their signal at an aperture of 8 and their signal at an aperture of 3. This relationship is only linear, however, if the bright stars are not saturating the CCD, so any stars from the selection that had saturated pixels were removed. Once a set of bright stars was chosen for each CCD, aperture photometry was performed on those stars in the 60s exposure images for each filter using a pixel radius of 3 and 8. To make the correction this formula was used

$$N_{\text{star},8/3} = \frac{N_{\text{star},8}}{N_{\text{star},3}} \tag{2.7}$$

for each star in the set where

$$\sigma^2_{N_{\text{star},8/3}} = \left(\frac{N_{\text{star},8}}{N_{\text{star},3}}\right)^2 \left[\left(\frac{\sigma_{N_{\text{star},8}}}{N_{\text{star},8}}\right)^2 + \left(\frac{\sigma_{N_{\text{star},3}}}{N_{\text{star},3}}\right)^2\right]. \tag{2.8}$$

A weighted average was taken of the correction term $N_{\text{star},8/3}$ of each star using

$$\langle N_{8/3} \rangle = \frac{\sum_{i=1}^{n} \frac{N_{\text{star},8/3}}{\sigma^2_{N_{8/3}}}}{\sum_{i=1}^{n} \frac{1}{\sigma^2_{N_{\text{star},8/3}}}} \tag{2.9}$$

to find a correction term that could be applied to all the stars in each CCD-filter combination. To find the error in the correction term this formula was used

$$\sigma^2_{\langle N_{\mathrm{star},8/3}\rangle} = \frac{1}{\sum_{i=1}^{N} \frac{1}{\sigma^2_{N_{\mathrm{star},8/3}}}}. \tag{2.10}$$

2.6 Sensitivities

Once the aperture correction was obtained, aperture photometry was performed on all the stars in the field using an aperture of radius 3 pixels. Using the sky values obtained for each image (see Sec. 2.3) the value of $N_{\mathrm{star}\ 3}$ for each star could be determined using Eq. 2.1. To find the corrected star counts at an aperture of 8 pixels this formula was used

$$N_{\mathrm{star},8,\mathrm{corrected}} = N_{\mathrm{star},3} * \langle N_{\mathrm{star},8/3}\rangle. \tag{2.11}$$

The error in the corrected star counts at an aperture of 8 is given by

$$\sigma^2_{N_{\mathrm{star},8,\mathrm{corrected}}} = N^2_{\mathrm{star},3} * \sigma^2_{\langle N_{\mathrm{star},8/3}\rangle} + \langle N_{\mathrm{star},8/3}\rangle^2 * \sigma^2_{N_{\mathrm{star},3}}. \tag{2.12}$$

With the corrected star counts the signal (S) was found by multiplying $N_{\mathrm{star},8,\mathrm{corrected}}$ by the gain (G) of the CCD. To find the noise (N), the following noise equation was used

$$N^2 = G * \sigma^2_{N_{\mathrm{star},8,\mathrm{corrected}}} + G * A_3 * \sigma^2_{\langle m_{\mathrm{sky}}\rangle} + A_3 * R^2, \tag{2.13}$$

where A_3 is the area of a 3 pixel radius aperture and R is the read noise of the CCD. Finally with signal and noise, magnitudes (M) and errors in those magnitudes, (σ_M) could be calculated. Magnitudes were found using Eq. 2.3. To find σ_M values of M_+ and M_- were created using

$$M_\pm = -2.5 * \log_{10}\left(\frac{S \pm N}{t}\right) + M_z. \tag{2.14}$$

These values were then plugged into

$$\sigma_M = \frac{M_- - M_+}{2}. \tag{2.15}$$

With the magnitudes and errors for the stars in the NGC 188 field, it was known how accurate each CCD was in each filter for each magnitude.

Chapter 3

Results

3.1 Zero Points

From the photometry performed on the Landolt standard stars in the SA 110 field the zero points listed in Table 3.1 were determined. These zero point magnitudes represent the magnitude of a stellar object that would make one count on a CCD per second. These zero point magnitudes make it possible to find the apparent magnitudes of stellar objects observed with the 0.9m telescope and associated CCD.

Table 3.1. Zero Points for Two CCDs Used at WMO

	B		V		R		I	
CCD	M_z	σ_{M_z}	M_z	σ_{M_z}	M_z	σ_{M_z}	M_z	σ_{M_z}
KAF-09000	21.6201	0.00120	22.0306	0.00108	22.0998	0.00071	21.0825	0.00082
3041-UV	22.8066	0.00162	22.7535	0.00168	22.8539	0.00122		

3.2 Sensitivities

The sensitivities listed in Tables 3.2 and 3.3 represent the capabilities of the KAF-09000 and 3041-UV CCDs when mounted on WMO's 0.9m telescope. As expected the S/N increases and σ_M decreases as the integration time t increases. So, as the CCD is exposed longer, it can detect fainter objects with more precision. These sensitivities also allow astronomers to select the correct exposure times to observe brightness variability as small as σ_M in stellar objects of magnitude M. This is most important for astronomers studying short-term variability; in order to see magnitude changes over a short period of time, exposure times must be short enough that images can be taken with enough frequency to see features of interest. These exposure times, however, cannot be too short, or the magnitude variability will be smaller than the variability caused by the noise. Since exoplanetary transits cause short-term variability in the stars they orbit, choosing the right exposure times requires knowledge of CCD sensitivities.

Table 3.2. Photometric Sensitivity of the KAF-09000 CCD

		B		V		R		I	
M	t[s]	S/N	σ_M	S/N	σ_M	S/N	σ_M	S/N	σ_M
9	60							1192.44	0.00091
	120								
	240								
	480								
	960								
10	60	784.24	0.00138	1148.36	0.00095	1367.33	0.00079	888.06	0.00123
	120	813.49	0.00133					1119.96	0.00097
	240								
	480								
	960								
11	60	651.29	0.00167	830.22	0.00131	982.24	0.00111	612.28	0.00177
	120	753.79	0.00144	1047.74	0.00104	1270.71	0.00085	804.38	0.00135
	240	813.43	0.00133	1159.04	0.00094			1015.87	0.00107
	480							1188.29	0.00091
	960								
12	60	478.58	0.00227	573.84	0.00189	652.90	0.00166	381.95	0.00284
	120	608.56	0.00178	775.66	0.00140	876.19	0.00124	543.77	0.00200
	240	719.49	0.00151	988.41	0.00110	1175.53	0.00092	731.61	0.00148
	480	809.27	0.00134	1152.19	0.00094			946.57	0.00115
	960							1169.29	0.00093
13	60	309.56	0.00351	360.52	0.00301	394.84	0.00275	225.27	0.00482
	120	423.87	0.00256	512.85	0.00212	559.05	0.00194	328.06	0.00331
	240	551.99	0.00197	687.54	0.00158	772.85	0.00140	465.72	0.00233

Table 3.2 (cont'd)

		B		V		R		I	
M	t[s]	S/N	σ_M	S/N	σ_M	S/N	σ_M	S/N	σ_M
	480	686.67	0.00158	904.52	0.00120	1041.94	0.00104	636.98	0.00170
	960	771.03	0.00141	1095.55	0.00099	1286.15	0.00084	839.57	0.00129
14	60	192.52	0.00564	205.34	0.00529	223.77	0.00485	119.57	0.00908
	120	278.29	0.00390	308.14	0.00352	321.47	0.00338	180.88	0.00600
	240	387.29	0.00280	437.43	0.00248	461.53	0.00235	263.09	0.00413
	480	510.84	0.00213	596.50	0.00182	646.41	0.00168	373.38	0.00291
	960	630.95	0.00172	779.53	0.00139	880.42	0.00123	508.44	0.00214
15	60	106.66	0.01018	106.44	0.01020	115.34	0.00941	56.93	0.01907
	120	160.32	0.00677	167.70	0.00647	169.08	0.00642	89.29	0.01216
	240	238.41	0.00455	246.36	0.00441	246.68	0.00440	133.73	0.00812
	480	336.17	0.00323	349.43	0.00311	355.63	0.00305	194.59	0.00558
	960	437.75	0.00248	451.06	0.00241	488.24	0.00222	264.88	0.00410
16	60	51.67	0.02101	48.99	0.02217	53.16	0.02042	24.90	0.04362
	120	81.53	0.01332	82.07	0.01323	79.33	0.01369	39.88	0.02723
	240	130.35	0.00833	123.56	0.00879	117.22	0.00926	61.16	0.01775
	480	190.10	0.00571	177.07	0.00613	171.53	0.00633	89.51	0.01213
	960	248.87	0.00436	225.88	0.00481	237.28	0.00458	121.54	0.00893
17	60	22.99	0.04726	21.11	0.05147	22.86	0.04752	10.27	0.10605
	120	36.97	0.02937	35.90	0.03025	34.25	0.03171	16.69	0.06514
	240	62.85	0.01728	55.50	0.01957	50.89	0.02134	25.84	0.04204
	480	94.03	0.01155	81.25	0.01336	75.35	0.01441	38.35	0.02832
	960	122.76	0.00884	100.42	0.01081	103.61	0.01048	52.03	0.02087
18	60	9.62	0.11326	8.65	0.12613	9.39	0.11611	3.98	0.27842

Table 3.2 (cont'd)

		B		V		R		I	
M	t[s]	S/N	σ_M	S/N	σ_M	S/N	σ_M	S/N	σ_M
	120	15.84	0.06862	15.23	0.07138	14.24	0.07639	7.24	0.15086
	240	27.63	0.03931	23.39	0.04646	21.20	0.05125	11.10	0.09810
	480	41.79	0.02598	34.26	0.03170	31.35	0.03465	15.11	0.07195
	960	53.61	0.02026	41.66	0.02607	43.12	0.02518	20.39	0.05330
19	60	3.90	0.28481	3.51	0.31787	3.72	0.33721	1.46	0.90909
	120	6.52	0.16781	6.16	0.17795	5.81	0.18881	2.53	0.45366
	240	11.54	0.09432	8.76	0.12441	8.17	0.13349	4.18	0.26510
	480	17.38	0.06254	14.16	0.07678	10.97	0.09925	5.98	0.18335
	960	22.30	0.04871	16.61	0.06543	12.54	0.08679	7.59	0.14388
20	60	1.56	0.82603	1.40	0.96896	1.41	0.96380	0.68	
	120	2.62	0.43671	2.66	0.42952	2.07	0.57340	1.05	2.02291
	240	4.64	0.23754	4.20	0.26330	2.90	0.38975	1.72	0.72178
	480	6.99	0.15645	8.00	0.18733	5.01	0.21964	2.29	0.50724
	960	8.95	0.12184	6.46	0.16946	6.78	0.16132	3.07	0.36753

Table 3.3. Photometric Sensitivity of the Fairchild 3041-UV CCD

		B		V		R	
M	t[s]	S/N	σ_M	S/N	σ_M	S/N	σ_M
11	60	619.69	0.00175				
	120						
	240						
	480						
	960						
12	60	559.72	0.00194	729.17	0.00149	918.65	0.00118
	120	616.07	0.00176	840.79	0.00129		
	240						
	480						
	960						
13	60	473.02	0.00230	551.97	0.00197	635.40	0.00171
	120	545.26	0.00199	691.38	0.00157	832.78	0.00130
	240	599.53	0.00181	805.56	0.00135	1020.02	0.00106
	480						
	960						
14	60	342.44	0.00317	361.63	0.00300	403.73	0.00269
	120	429.68	0.00253	486.82	0.00223	558.01	0.00195
	240	517.39	0.00210	628.19	0.00173	733.26	0.00148
	480	577.03	0.00188	755.45	0.00144	932.00	0.00116
	960						
15	60	212.08	0.00512	207.18	0.00524	220.87	0.00492
	120	285.43	0.00380	299.40	0.00363	316.50	0.00343
	240	384.08	0.00283	417.96	0.00260	442.56	0.00245

Table 3.3 (cont'd)

		B		V		R	
M	t[s]	S/N	σ_M	S/N	σ_M	S/N	σ_M
	480	469.35	0.00231	552.23	0.00197	612.82	0.00177
	960	530.77	0.00205	640.03	0.00170	721.57	0.00150
16	60	113.98	0.00953	103.26	0.01051	107.40	0.01011
	120	159.06	0.00683	157.39	0.00690	160.65	0.00676
	240	231.11	0.00470	231.46	0.00469	224.57	0.00483
	480	306.08	0.00355	326.49	0.00333	331.93	0.00327
	960	373.09	0.00291	374.85	0.00290	377.27	0.00288
17	60	53.84	0.02017	46.36	0.02342	47.44	0.02289
	120	76.05	0.01428	72.47	0.01498	72.73	0.01493
	240	116.05	0.00936	109.08	0.00995	101.91	0.01065
	480	159.69	0.00680	161.27	0.00673	154.67	0.00702
	960	199.02	0.00546	176.59	0.00615	168.79	0.00643
18	60	23.20	0.04683	19.45	0.05587	19.82	0.05482
	120	33.09	0.03282	31.04	0.03499	30.68	0.03541
	240	51.49	0.02109	47.76	0.02274	43.08	0.02521
	480	71.63	0.01516	71.10	0.01527	66.36	0.01636
	960	87.89	0.01235	75.24	0.01443	70.42	0.01542
19	60	9.56	0.11403	8.00	0.13650	8.05	0.13550
	120	13.70	0.07938	12.68	0.08583	12.28	0.08858
	240	21.79	0.04986	19.69	0.05518	17.49	0.06214
	480	29.74	0.03652	29.42	0.03692	27.19	0.03995
	960	36.34	0.02989	30.39	0.03573	28.33	0.03834
20	60	3.89	0.28531	3.23	0.34733	3.06	0.36854

Table 3.3 (cont'd)

		B		V		R	
M	t[s]	S/N	σ_M	S/N	σ_M	S/N	σ_M
	120	5.51	0.19925	5.13	0.21437	5.44	0.20202
	240	8.77	0.12432	7.88	0.13849	7.14	0.15304
	480	12.16	0.08950	10.96	0.09930	10.66	0.10327
	960	14.74	0.07376	12.31	0.08836	11.21	0.09708
21	60	1.55	0.83137	1.25	1.19462	1.20	1.29115
	120	2.21	0.53068	1.89	0.63815	1.96	0.61076
	240	3.54	0.31492	3.32	0.33775	2.76	0.41244
	480	4.90	0.22472	4.73	0.23293	4.40	0.25090
	960	5.92	0.18525	4.91	0.22432	4.70	0.23449

3.3 Integration Times

Since BYU will be studying the exoplanets from the Kepler exoplanet candidate list, the sensitivities listed in Tables 3.2 and 3.3 can provide information on how to observe the planetary transits. For example, let Kepler-x be an exoplanet candidate found by the NASA Kepler mission. If Kepler-x orbits a host star of V magnitude 15, and causes its host star to drop in magnitude by 0.004, what would be the shortest exposure time that would still allow the transit to be seen? With the KAF-09000 CCD, exposure times must be greater than 480s to notice magnitude changes as small as 0.004. Using the 3041-UV CCD, exposure times must be greater than 120s. Depending on the length of Kepler-x's transit, exposure times longer than the minimum would reduce the noise in the data without affecting the resolution of the transit light curve. However, if exposure times are increased too much, resolution of the light curve could be jeopardized by having too few data points to accurately find the start, middle, and end of the transit.

3.4 Conclusions

Using the results obtained in this thesis BYU will be able to go forward with its study of exosolar planets. These results can help dictate decisions about the length of observational exposure times and the viability of candidates for research using the 0.9m WMO telescope. The next step in BYU's study of exoplanets is to take observations of the exoplanet candidates released by the NASA Kepler Mission. By studying the host star's light curve, BYU's Department of Physics and Astronomy may be the next research group to announce the discovery of an exoplanet.

Appendix A

Error Propagation

In order to obtain the sensitivities of the telescope, it was necessary to properly propagate the error so the signal-to-noise ratio and error in magnitude could be calculated for each magnitude. This appendix lists the error propagation formulas used.

Weighted Average:

$$\langle x \rangle = \frac{\sum_{i=1}^{n} \frac{x_i}{\sigma_x^2}}{\sum_{i=1}^{n} \frac{1}{\sigma_{x_i}^2}} \tag{A.1}$$

Variance of the Weighted Average:

$$\sigma_{\langle x \rangle}^2 = \frac{1}{\sum_{i=1}^{n} \frac{1}{\sigma_{x_i}^2}} \tag{A.2}$$

Error Propagation in Addition and Subtraction

$$\sigma_{A \pm B}^2 = \sigma_A^2 + \sigma_B^2 \tag{A.3}$$

Error Propagation in Multiplication and Division

$$\sigma_{A*B}^2 = (A*B)^2 \left[\left(\frac{\sigma_A}{A} \right)^2 + \left(\frac{\sigma_B}{B} \right)^2 \right] \tag{A.4}$$

$$\sigma_{A/B}^2 = (A/B)^2 \left[\left(\frac{\sigma_A}{A} \right)^2 + \left(\frac{\sigma_B}{B} \right)^2 \right] \tag{A.5}$$

Bibliography

Borucki, W. J., et al. 2011, Am. J. Phys., 736, 19

Howell, S. B. 2006, Handbook of CCD Astronomy, 2nd edn. (United Kingdom: Cambridge University Press)

Landolt, A. U. 1973, The Astronomical Jounal, 78, 959

Tody, D. 1993, in Astronomical Society of the Pacific Conference Series, Vol. 52, Astronomical Data Analysis Software and Systems II, ed. . J. B. R. J. Hanisch, R. J. V. Brissenden, 173